Impact of Assimilating Ocean Velocity Observations Inferred from Lagrangian Drifter Data Using the NCOM-4DVAR*

MATTHEW J. CARRIER, HANS NGODOCK, SCOTT SMITH, AND GREGG JACOBS

Naval Research Laboratory, Stennis Space Center, Mississippi

PHILIP MUSCARELLA

American Society for Engineering Education, Washington, D.C.

TAMAY OZGOKMEN AND BRIAN HAUS

University of Miami, Miami, Florida

BRUCE LIPPHARDT

University of Delaware, Newark, Delaware

(Manuscript received 23 July 2013, in final form 6 November 2013)

ABSTRACT

Eulerian velocity fields are derived from 300 drifters released in the Gulf of Mexico by The Consortium for Advanced Research on Transport of Hydrocarbon in the Environment (CARTHE) during the summer 2012 Grand Lagrangian Deployment (GLAD) experiment. These data are directly assimilated into the Navy Coastal Ocean Model (NCOM) four-dimensional variational data assimilation (4DVAR) analysis system in a series of experiments to investigate their impact on the model circulation. The NCOM-4DVAR is a newly developed tool for data analysis, formulated for weak-constraint data assimilation based on the indirect representer method. The assimilation experiments take advantage of this velocity data along with other available data sources from in situ and satellite measurements of surface and subsurface temperature and salinity. Three different experiments are done: (i) A nonassimilative NCOM free run, (ii) an assimilative NCOM run that utilizes temperature and salinity observations, and (iii) an assimilative NCOM run that uses temperature and salinity observations as well as the GLAD velocity observations. The resulting analyses and subsequent forecasts are compared to assimilated and future GLAD velocity and temperature/salinity observations to determine the performance of each experiment and the impact of the GLAD data on the analysis and the forecast. It is shown that the NCOM-4DVAR is able to fit the observations not only in the analysis step, but also in the subsequent forecast. It is also found that the GLAD velocity data greatly improves the characterization of the circulation, with the forecast showing a better fit to future GLAD observations than those experiments without the velocity data included.

1. Introduction

Modern ocean forecasting using numerical models has advanced significantly in the past 20 years. Models, such as the Princeton Ocean Model (POM; Blumberg and Mellor 1987), the Regional Ocean Modeling System (ROMS; Shchepetkin and McWilliams 2003, 2005; Marchesiello et al. 2001), the Navy Coastal Ocean Model (NCOM; Martin 2000; Barron et al. 2006), and the Hybrid Coordinate Ocean Model (HYCOM; Bleck 2002) are capable of producing very accurate ocean simulations for regional and global applications at resolutions ranging from tens of kilometers to a few hundred meters. Despite recent advancement, numerical modeling continues to suffer from inherent errors associated with unresolved processes, inaccurate parameterizations,

*Naval Research Laboratory Contribution Number JA/7320-13-1824.

Corresponding author address: Matthew J. Carrier, Naval Research Laboratory, Bldg. 1009, Balch Blvd., Stennis Space Center, MS 39529.
E-mail: matthew.carrier@nrlssc.navy.mil

DOI: 10.1175/MWR-D-13-00236.1

Report Documentation Page

Form Approved
OMB No. 0704-0188

1. REPORT DATE	2. REPORT TYPE	3. DATES COVERED
APR 2014		**00-00-2014 to 00-00-2014**

4. TITLE AND SUBTITLE	5a. CONTRACT NUMBER
Impact of Assimilating Ocean Velocity Observations Inferred from Lagrangian Drifter Data Using the NCOM-4DVAR	5b. GRANT NUMBER
	5c. PROGRAM ELEMENT NUMBER
6. AUTHOR(S)	5d. PROJECT NUMBER
	5e. TASK NUMBER
	5f. WORK UNIT NUMBER
7. PERFORMING ORGANIZATION NAME(S) AND ADDRESS(ES) **Naval Research Laboratory,Bldg. 1009, Balch Blvd,Stennis Space Center,MS,39529**	8. PERFORMING ORGANIZATION REPORT NUMBER
9. SPONSORING/MONITORING AGENCY NAME(S) AND ADDRESS(ES)	10. SPONSOR/MONITOR'S ACRONYM(S)
	11. SPONSOR/MONITOR'S REPORT NUMBER(S)

12. DISTRIBUTION/AVAILABILITY STATEMENT
Approved for public release; distribution unlimited

13. SUPPLEMENTARY NOTES

14. ABSTRACT

Eulerian velocity fields are derived from 300 drifters released in the Gulf of Mexico by The Consortium for Advanced Research on Transport of Hydrocarbon in the Environment (CARTHE) during the summer 2012 Grand Lagrangian Deployment (GLAD) experiment. These data are directly assimilated into the Navy Coastal Ocean Model (NCOM) four-dimensional variational data assimilation (4DVAR) analysis system in a series of experiments to investigate their impact on the model circulation. The NCOM-4DVAR is a newly developed tool for data analysis, formulated for weak-constraint data assimilation based on the indirect representer method. The assimilation experiments take advantage of this velocity data along with other available data sources from in situ and satellite measurements of surface and subsurface temperature and salinity. Three different experiments are done: (i) A nonassimilative NCOM free run, (ii) an assimilative NCOM run that utilizes temperature and salinity observations, and (iii) an assimilative NCOM run that uses temperature and salinity observations as well as the GLAD velocity observations. The resulting analyses and subsequent forecasts are compared to assimilated and future GLAD velocity and temperature/salinity observations to determine the performance of each experiment and the impact of the GLAD data on the analysis and the forecast. It is shown that the NCOM-4DVARis able to fit the observations not only in the analysis step, but also in the subsequent forecast. It is also found that the GLAD velocity data greatly improves the characterization of the circulation, with the forecast showing a better fit to future GLAD observations than those experiments without the velocity data included.

15. SUBJECT TERMS

16. SECURITY CLASSIFICATION OF:			17. LIMITATION OF ABSTRACT	18. NUMBER OF PAGES	19a. NAME OF RESPONSIBLE PERSON
a. REPORT **unclassified**	b. ABSTRACT **unclassified**	c. THIS PAGE **unclassified**	**Same as Report (SAR)**	**16**	

errors in specified surface and/or boundary conditions, and errors in the initial conditions. As such, if a model simulation were to continue uncorrected, the forecast trajectory will inevitably veer away from reality as the effects of these errors accumulate.

Because of the impact of model error, frequent updating of the model trajectory from available observations is a key component of any ocean or atmospheric forecasting system. Data assimilation (DA) provides the means to produce suitable state estimation from which the model can be periodically adjusted to move the forecast trajectory closer to reality. For ocean forecasting, this need is important when attempting to accurately simulate ocean currents at regional scales. On large scales, existing ocean models do an adequate job of resolving the oceanic flow from the placement of the Gulf Stream to the Kuroshio. However, at regional and mesoscales, where the prediction of individual tracers or drifters are important for search and rescue operations or hydrocarbon/chemical spill simulations, the ocean models lack sufficient accuracy; therefore, it is important to be able to properly constrain the model simulation, at the prescribed resolution, with actual observations of ocean current velocities.

There has been some work in the area of assimilating ocean velocity observations to improve the characterization of model currents. These have taken the form of simple nudging methods (Fan et al. 2004) to the more complex variational methods (Taillandier et al. 2006; Nilsson et al. 2012). Ocean velocity DA has also seen variety regarding the form of the observation to be used, specifically Lagrangian (i.e., following the flow) or Eulerian (stationary). Traditional Eulerian measurements consist of point measurements from acoustic Doppler current profilers (ADCP) or high-frequency (HF) radar surface current measurements that measure the speed and direction of the ocean currents at a fixed location in space. Lagrangian data are collected from data-gathering devices on board any passive tracer, such as drifters or surface floats. Eulerian observations can be assimilated directly into the ocean model as the form of the data matches that of the model variable. Lagrangian data, on the other hand, must be handled differently as the data here consists of position—time measurements, not ocean velocity directly. There have been numerous attempts to assimilate Lagrangian data, either by deriving Eulerian velocity from the dataset by calculating the change in drifter position over some time scale (Hernandez et al. 1995; Ishikawa et al. 1996), or by assimilating the Lagrangian data directly by evolving a series of tracers within the model simulation then minimizing the distance between the observed and model tracers via some DA scheme (Molcard et al. 2003; Ozgokmen et al. 2003; Taillandier et al. 2006; Nilsson et al. 2012), or by state augmentation via a Kalman filter scheme (Ide et al. 2002; Kuznetsov et al. 2003; Salman et al. 2006). Molcard et al. (2005) point out that the former method, dubbed ''pseudo-Lagrangian,'' can be problematic if the data sampling period exceeds the Lagrangian time scale, which is usually on the order of 1–3 days for ocean surface velocity measurements and 7–15 days for the ocean interior.

For this work, deriving Eulerian velocity measurements from the drifter positions from the Grand Lagrangian Deployment (GLAD) experiment is not problematic, as the sampling time is every 5 min (Pojc et al. 2013, manuscript submitted to *Nature*); therefore, derivation of reasonably accurate Eulerian velocities is possible. This effort aims to assess the impact of Eulerian velocity data, derived from the GLAD drifter locations, on a simulation of the Gulf of Mexico using NCOM. These observations are assimilated via the four-dimensional variational data assimilation (4DVAR) representer method (Bennett 1992, 2002; Chua and Bennett 2001; Kurapov et al. 2009, 2011) employed by the NCOM-4DVAR (Ngodock and Carrier 2013). These observations, along with available remote and in situ observations of temperature and salinity are used to initialize a series of 4-day forecasts. These analyses and forecasts are examined by comparison to future GLAD-derived Eulerian velocity observations and traditional temperature/salinity observations in an attempt to evaluate the impact of the assimilated velocities on the analyses and subsequent forecasts.

This paper is organized in the following manner: section 2 provides a discussion of the forecast model and the accompanying assimilation system; section 3 provides an overview of the GLAD experiment as well as the data processing methodology used to derive Eulerian values from the drifter position data; section 4 presents the design of the experiments used to evaluate the impact of the GLAD data on the ocean analysis and forecast; section 5 provides a discussion of the experiment results followed by a general summary and a discussion of future work in section 6.

2. Forecast model and analysis system

a. The Navy Coastal Ocean Model (NCOM)

NCOM is selected as the ocean forecast model for this work and is capable of producing forecasts of temperature, salinity, ocean currents, and sea surface height for regional and global applications. It is a primitive equation model with a free-surface and a generalized vertical coordinate that can be configured with terrain-following free-sigma or fixed-sigma, or constant z-level surfaces in

a number of combinations (Barron et al. 2006). The model employs the Mellor–Yamada level-2.5 turbulence closure parameterization (Mellor and Yamada 1982) for vertical diffusion and the Smagorinsky scheme (Smagorinsky 1963) for horizontal diffusion.

The model domain for this experiment extends from 18°–31°N to 79°–98°W using a spherical coordinate projection at a horizontal resolution of 6 km. The model has 50 layers in the vertical, with 25 free-sigma levels extending to a depth of 116 m with constant z-levels extending down to a maximum of 5500 m with the depth of the first subsurface layer at 0.5 m. The model resolution is coarse compared to other simulations of the Gulf of Mexico, but was necessary because of the computational expense of the NCOM-4DVAR, which can be many times more expensive than the forward model (Ngodock and Carrier 2013). Lateral boundary conditions are provided by the global NCOM model at 1/8° resolution (every 3 h) and surface atmospheric forcing, such as wind stress, atmospheric pressure, and surface heat flux is provided by the 0.5° Navy Operational Global Atmospheric Prediction System (NOGAPS) model every 3 h (Rosmond et al. 2002); river forcing is provided at all river in-flow locations in the Gulf of Mexico domain.

b. *The NCOM four-dimensional variational assimilation system (NCOM-4DVAR)*

The DA system selected for this work is the NCOM-4DVAR developed using the dynamical core of the forward NCOM model. The NCOM-4DVAR is a variational assimilation system based on the indirect representer method as described by Bennett (1992, 2002) and Chua and Bennett (2001). This system has been described in detail by Ngodock and Carrier (2013), and a full derivation of the representer method can be found in Chua and Bennett (2001), therefore, only an overview is provided here. The representer method aims to find an optimal analysis solution as the linear combination of a first guess (i.e., prior model solution) and a finite number of representer functions, one per datum

$$\hat{u}(x,t) = u_F(x,t) + \sum_{m=1}^{M} \hat{\beta}_m r_m(x,t), \qquad (1)$$

where $\hat{u}(x, t)$ is the optimal analysis solution, $u_F(x, t)$ is the prior forecast, $r_m(x, t)$ is the representer function for the mth observation, and $\hat{\beta}_m$ is the mth representer coefficient. The representer coefficients can be found by solving the linear system:

$$(\mathbf{R} + \mathbf{O})\beta = \mathbf{y} - \mathbf{H}\mathbf{x}^f, \qquad (2)$$

where $\mathbf{O}$ is the observation error covariance, $\mathbf{y}$ is the observation vector, $\mathbf{H}$ is the linear observation operator that maps the model fields to the observation locations, $\mathbf{x}^f$ is the model vector, and $\mathbf{R}$ is the representer matrix and is equivalent to $\mathbf{HMBM}^{\mathrm{T}}\mathbf{H}^{\mathrm{T}}$ ($\mathbf{M}$ is the tangent linear model, or TLM; $\mathbf{M}^{\mathrm{T}}$ is the adjoint of NCOM; $\mathbf{B}$ is the model error covariance; and T denotes the linear transposition). Since the matrix $\mathbf{R} + \mathbf{O}$ is symmetric and positive definite, (2) can be solved for β iteratively using a linear solver, such as the conjugate gradient method. From (2) it is clear that the $\hat{\beta}_m$ for each representer can be found by integrating the adjoint and TLM over some number of minimization steps until convergence. Once found, $\hat{\beta}_m$ is acted upon by (1), involving one final sweep through the adjoint and TLM to find the optimal correction.

In the NCOM-4DVAR, $\hat{\beta}_m$ is found with a preconditioned conjugate gradient solver. The preconditioner here follows from Courtier (1997) to introduce a change of variable in the minimization step described in (2), where β is redefined as $\mathbf{u} = \sqrt{\mathbf{O}}\beta$ so that (2) can now be expressed as

$$(\sqrt{\mathbf{O}^{-1}}\mathbf{R}\sqrt{\mathbf{O}^{-1}} + \mathbf{I})\mathbf{u} = \sqrt{\mathbf{O}^{-1}}(\mathbf{y} - \mathbf{H}\mathbf{x}^f). \qquad (3)$$

This transformation ensures that there is a lower bound of 1 for the eigenvalues, which ensures that the condition number will remain reasonably small.

The background and model error covariance in NCOM-4DVAR follow the work of Weaver and Courtier (2001) and Carrier and Ngodock (2010) where the error covariance is univariate. This is deemed acceptable as the application of the tangent linear and adjoint models in the minimization and final sweep provide multivariate balance constraints through the linearized dynamics. It has been shown (Yu et al. 2012) that omitting linear balance constraints does not lead to a significant degradation of the final solution in terms of the fit to observations. The univariate error covariance can be further decomposed into a correlation matrix and the associated error variance such that

$$\mathbf{B} = \mathbf{\Sigma}\mathbf{C}\mathbf{\Sigma}, \qquad (4)$$

where $\mathbf{\Sigma}$ is a diagonal matrix of the error standard deviation and $\mathbf{C}$ is a symmetric matrix of error correlations. In NCOM-4DVAR the error standard deviations of the background are used at the initialization of the tangent linear model only, whereas the model error (also contained in the matrix $\mathbf{\Sigma}$) is used when the adjoint forces the tangent linear model during integration (i.e., as the tangent linear model integrates forward in time). This

allows the weak constraint method to correct for the initial condition error while also adjusting the forward model trajectory based on the specification of the model error. The error correlation, for both the model and the background errors are not directly calculated and stored in NCOM-4DVAR; rather, the *effect* of the correlation matrix acting on an input vector is modeled by the solution of a diffusion equation following the work of Weaver and Courtier (2001). For a full explanation of this method, we refer the reader to Weaver and Courtier (2001) or Yaremchuk et al. (2013); for a description of the implementation of this method in NCOM-4DVAR, we refer the reader to Carrier and Ngodock (2010) or Ngodock (2005).

3. Data and processing

With a Gulf of Mexico Research Initiative (GoMRI) award, the Consortium for Advanced Research on Transport of Hydrocarbons in the Environment (CARTHE) conducted an unprecedented large-scale deployment of 300 custom-built drifters in the northern Gulf of Mexico in the summer of 2012. Equipped with GPS positioning, the drifters are capable of reporting their positions every 5 min, allowing for excellent temporal resolution and for accurate estimates of the Eulerian velocity along the drifter track. The drifters are drogued to a depth of 1 m (Pojc et al. 2013, manuscript submitted to *Nature*).

Although the NCOM-4DVAR system can be adapted to assimilate drifter positions because of the available adjoint of the momentum equation, it is decided for the sake of convenience to use the drifter data to estimate the Eulerian velocities, which could be more easily assimilated into the model using the existing assimilation architecture without the need to update or alter the existing forward, tangent linear, and adjoint codes. The basic principle behind the derivation of Eulerian velocity from a Lagrangian data source involves the calculation of the distance traveled by the drifter over some time scale. In practice, however, the calculation is more complicated due to noisy position values and nonphysical accelerations, such as a drifter being removed from the water by the crew of a passing ship. The GLAD drifter observations are highly nonstationary, and therefore, can simultaneously represent multiple scales at once. This makes filtering the observations very difficult, because filtering the larger scales of motion will overly smooth the small-scale velocity values. Therefore, a multistep process is used to derive Eulerian velocities from the GLAD drifter position data. First, the instantaneous velocity and its associated acceleration vector (i.e., change in instantaneous velocity from one velocity location to the next) are computed. The algorithm cancels any data point where the velocity magnitude exceeds the threshold maximum of $3\,\mathrm{m\,s^{-1}}$ or if the data rotation exceeds the maximum threshold of $2\pi\,(3\,\mathrm{h})^{-1}$. No subsequent data from a particular drifter are included in the processing if the drifter travels more than 80 km in 12 h, or if the drifter travels less than 100 m in 12 h. The remaining velocities are sampled at the smallest possible constant interval and are filtered to remove high-frequency noise (cutoff of $2 \times$ Nyquist, roughly 1/10 min). The velocity values are then computed at each remaining position and the data are stored.

In addition to the derived Eulerian velocity data, other available sources of data are used in this study. Both remotely sensed and in situ ocean observation data are assimilated from (Geostationary Operational Environmental Satellite) GOES-East sea surface temperatures (SSTs), Argo profiling floats (Roemmich et al. 2001), expendable bathythermographs (XBT), and drifting buoys. These data are gathered and quality controlled using the operational data preparation utility from the Navy Coupled Ocean Data Assimilation (NCODA) system (Cummings 2005). These data are collected, preprocessed and used within the NCOM-4DVAR assimilation window at their respective observation times. It should be noted that no altimeter data are assimilated in this work. This is done in order to properly evaluate the impact of the velocity observations in the assimilation. Since altimeter observations help constrain the mesoscale features, it can be used to correct ocean velocity as well. In this present work, corrections made to the mesoscale features and the ocean velocity can be directly attributed to the assimilation of the drifter observations alone.

4. Experiment design

The forecast and analysis experiments are conducted to ascertain the impact of the GLAD data on the NCOM forecast and to determine if their inclusion within the data stream improves the forecast of near-surface ocean currents. The experiments shown in this work cover the time period between 1 August and 30 September 2012 and are located in the region where the GLAD drifters are deployed during this time frame. During this time, the loop current has already shed an eddy that is located, for the majority of the experiment, near the central Gulf of Mexico. Figure 1 (left panel) shows a composite image of sea surface height (SSH) observations taken from the available altimeters between 20 and 30 September 2012 and processed by the NCODA data preparatory suite. The estimated heights are shown here, not the anomalies, for a more direct comparison to the model

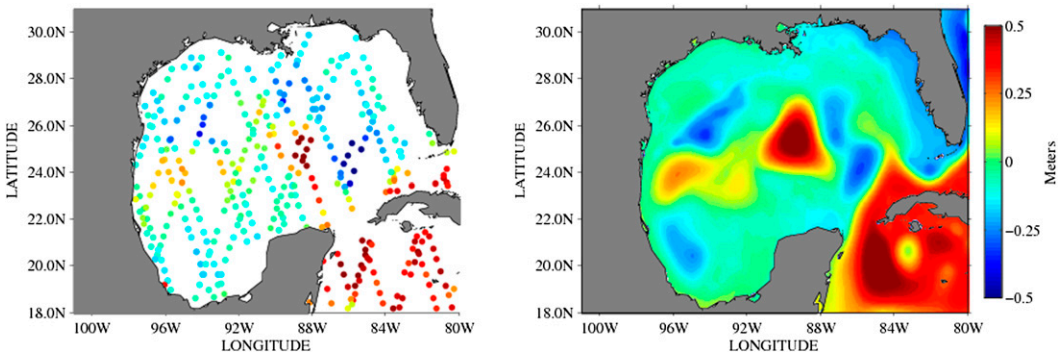

FIG. 1. (left) Composite of observed sea surface height (SSH) values from 20 to 30 Sep 2012 (value of the observation indicated by color bar in meters). (right) NCOM model SSH solution, valid 30 Sep 2012.

SSH field, shown in Fig. 1 (right panel). This model SSH field is valid on 30 September 2012 (taken from a free-run NCOM solution). To estimate the sea surface height from the observation data, a long-term mean SSH field from HYCOM has been interpolated to the observation locations and added to the anomalies. Figure 1 indicates that the loop current has shed an eddy, now located near the central Gulf of Mexico. The NCOM solution in Fig. 1 shows that the forecast model has captured the general location of the eddy and its separation from the loop current, although the shape and positioning does not exactly match the altimeter data (its position being offset to the west from the observations).

The location of the GLAD drifter observations covers much of the central Gulf of Mexico throughout the experiment time frame. Figure 2 shows the location of the processed GLAD drifter velocity data from 1 August to 30 September 2012 (positions plotted daily). It can be seen in Fig. 2 that the GLAD drifter velocity data has a high concentration of observations near the northern Gulf Coast, but still with good coverage farther south near the loop current and the region of the loop current eddy.

a. Analysis procedure

For this study, the observations are assimilated in a weak-constraint mode in order to have full control over the correction of the model trajectory and to attempt to account for sources of model error that we believe have the largest contribution to the forecast error in surface current velocity. The initial condition error for each of the following experiments is set as 2.0°C for temperature, 0.5 practical salinity unit (psu) for salinity, $0.2\,\mathrm{m\,s^{-1}}$ for velocity, and 0.1 m for SSH. These errors have been set by examining the innovation values of the 96-h forecasts from the free-running NCOM model as compared to available observations. The 96-h forecast is used to estimate the initial condition error due to the update cycle employed in this work (see section 4b). These values are uniform across the ocean model domain, mainly to aid in the convergence rate of the assimilation system, but also the values set here are representative of the average error across the domain. These values are reduced at depth as $\exp(z/z_0)$, where $z_0 = 1000\,\mathrm{m}$ and z is 0 at the surface and negative at depth (Yu et al. 2012). This is deemed acceptable as it is not expected that the ocean model will be largely in error at depth, especially considering that we are mostly interested in the accuracy of surface currents. The model errors are assumed to be due to errors in the specified atmospheric surface forcing for this study. This is deemed reasonable as ocean currents at the surface are strongly affected by surface wind stress. As such, the errors are assumed to be 10% of the average value of each surface forcing field through the assimilation window, which corresponds to roughly $40\,\mathrm{W\,m^{-2}}$ for the combined solar and temperature fluxes, 0.25 Pa for the surface wind stress, and $4.0 \times 10^{-7}\,\mathrm{psu\,m\,s^{-1}}$ for the surface salinity flux. These error values are then converted to the units of the ocean model variables (i.e.,

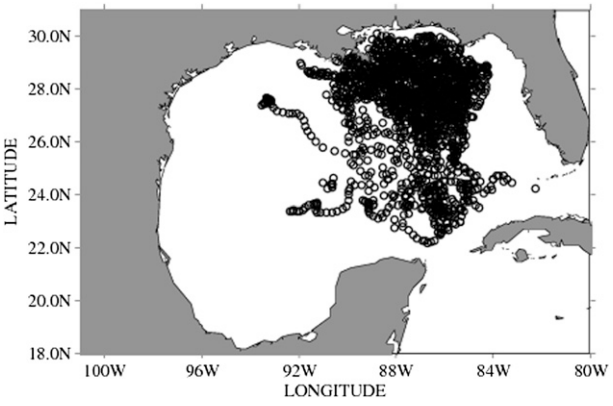

FIG. 2. Location of each GLAD drifter velocity observation from 1 Aug to 30 Sep 2012 (observations plotted at daily intervals).

heat flux to ocean temperature, wind stress to ocean velocity) and applied directly to the ocean variables of temperature, salinity, and velocity. The scale of the initial and model errors is taken to be roughly equivalent to the Rossby radius of deformation, which for the Gulf of Mexico ranges between 30 and 40 km and is fixed in time. Although the background error scales are static in time, the time-evolving, flow-dependent scales are applied via the dynamics provided by the tangent linear and adjoint of NCOM.

Each of the observations is also assigned errors. In operational data assimilation, the observation error is a combination of the estimated instrument error and the assumed representative error, with the latter set to account for features that may be present in the dataset that the model does not resolve. For this experiment each observation is assigned a static error that does not vary in space or time, again to aid in the convergence of the assimilation system. The temperature and salinity observation errors are representative of the values produced by the operational data processing system employed by the U.S. Navy. The errors are set as 0.2°C for temperature, 0.1 psu for salinity, and 0.02 m s^{-1} for velocity. The velocity error is found as a consequence of the GLAD data processing. The dataset used to compute the velocities for this work was the 15-min interval dataset derived from the GLAD position data. The drifter position error is estimated at 10 m. The corresponding velocity error is taken as the sum of the two position data points (~20 m) divided by the time interval between them (900 s). This yields a velocity error of about 0.02 m s^{-1}.

b. Selected experiments

Each experiment proceeds as a series of 4-day windows from 1 August to 30 September 2012. At the end of each 4-day assimilation window, the forecast model is run from the updated initial condition to provide the background for the next 4-day assimilation period. A free-run forecast (i.e., no assimilation) is also run in order to compare the assimilation analysis and forecast to a control to evaluate the impact of the assimilated observations. In a series of preliminary experiments (not shown), an attempt was made to evaluate the impact of the temporal frequency at which the observations are sampled for the assimilation. Three individual tests were done, each consisting of one 4-day assimilation cycle and subsequent 4-day forecast in which only the data sampling is varied while ingesting available observations every 6 h, 3 h, and hourly to determine which is the best setting for this study. It was determined that sampling observations every hour provides the best quality in terms of analysis fit to the observations as well as subsequent improvement to the forecast; the increased computational burden over less frequent observation input is minimal. It is interesting to note that this test illuminates the need for a larger number of velocity measurements in the assimilation step to ensure a good analysis and forecast fit to the observations. This is not surprising, however, as the ocean velocity is highly variable in time and space; therefore, more data are needed to properly constrain the model. All subsequent experiments shown, therefore, employ the hourly sampling strategy.

Two primary experiments are carried out to evaluate the impact of the GLAD velocity observations on the NCOM-4DVAR analysis and subsequent NCOM forecast. These experiments are (i) a cycling analysis/forecast run from 1 August to 30 September 2012 that uses the NCOM-4DVAR to assimilate temperature and salinity observations only (hereafter referred to as TS) and (ii) a cycling analysis/forecast run from 1 August to 30 September where temperature and salinity observations are assimilated along with the GLAD velocity observations by the NCOM-4DVAR analysis system (hereafter referred to as ALL). The analyses of each of these experiments are compared to the assimilated data to evaluate the performance of the assimilation in terms of the fit to the observations. The subsequent forecast from each analysis is compared to unassimilated data in the next analysis window (data that have yet to be assimilated, i.e., examining the innovations prior to assimilation). Theoretically, as data are assimilated by the system, the subsequent forecasts should be improved and, therefore, the size of the innovations in each subsequent assimilation window will be smaller; this is examined in this study.

5. Results

As a first-order evaluation of the impact of velocity data on the assimilation, the analysis fit to the assimilated observations is examined. Typically, a variational assimilation system should fit each of the assimilated observations to within one standard deviation of the observation error. To determine whether this criteria is met for this work, a normalized error metric is introduced as

$$J_{\text{fit}} = \frac{1}{M} \sum_{m=1}^{M} \frac{|\mathbf{y}_m - H_m \mathbf{X}^a|}{\sigma_m}, \tag{5}$$

where $\mathbf{y}_m$ is the mth observation, $\mathbf{X}^a$ is the analysis vector in model space (H_m maps the model analysis to the observation location), σ_m is the error standard deviation of the mth observation, and M is the total number of observations. By (5), if the analysis residual is within the

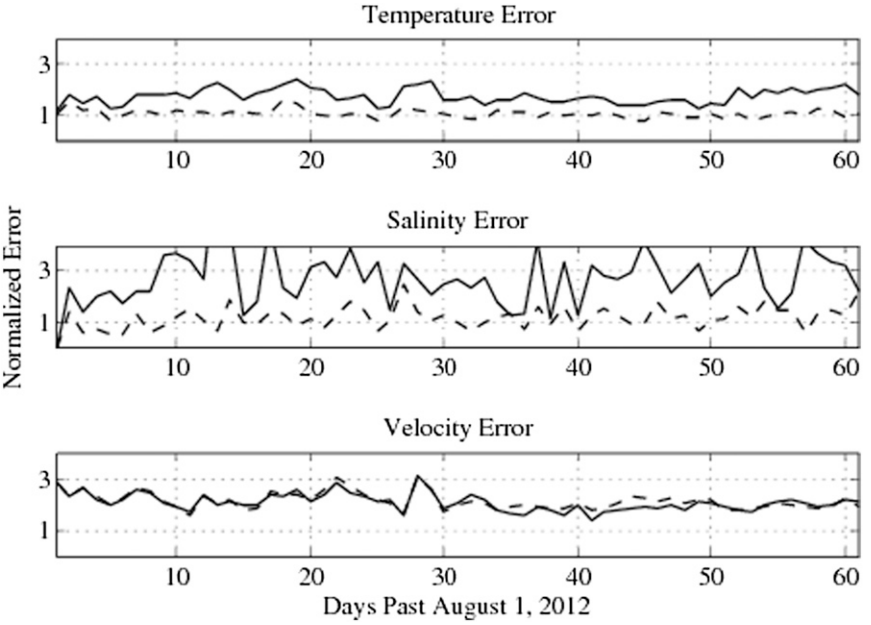

FIG. 3. The J_{fit} metric values for the NCOM free-run (FR) model solution (solid line) and TS analysis solution (dashed line) measured against (top) assimilated temperature observations, (middle) salinity observations, and (bottom) GLAD velocity observations. Valid from 1 Aug to 30 Sep 2012.

prescribed observation error, the J_{fit} value should be at or below 1.

Figure 3 shows the J_{fit} value for the temperature (top panel), salinity (middle panel), and velocity (bottom panel) observations from 1 August to 30 September, 2012; here the temperature and salinity observations are assimilated, but velocity is not. Two experiment results are shown in Fig. 3: the free-run (FR) NCOM background (solid) and the TS analysis (dash). This comparison is made to determine if the assimilation of temperature and salinity observations improve the analysis compared to the free-run solution.

Figure 3 shows that the assimilation of temperature and salinity has greatly improved the observation fit over that of the FR background, fitting both observation types generally within the prescribed observation error. The fit to velocity, here an independent data as the TS experiment does not assimilate velocity, shows no improvement in the representation of the surface velocity over that of the FR background. As one would expect, this indicates that the assimilation of temperature and salinity alone is not enough to correct the ocean velocity field. One can examine the analysis in regards to withheld observations as well. Because of the coarse resolution of the forecast model grid, it is possible to withhold a set of observations for each data type; in this case, the available observations are thinned by removing those observations that are considered redundant (i.e., within or at one correlation scale distance to an assimilated observation). A subset of observations can be collected from these withheld data to be used as further validation of the analysis. Here, only those withheld observations at a distance of at least 30–40 km from an assimilated observation are considered; all withheld observations that are at a distance less than this threshold are not used in this evaluation. These data may not necessarily represent purely independent observations; however, evaluating the analysis against these observations does provide insight as to the performance of the assimilation far from the location of included observations. Figure 4 shows the J_{fit} value of FR (solid) background and TS (dash) analysis to these withheld observations. The fit to temperature is not quite as good as to the assimilated observations, however, the TS analysis still shows some improvement over the FR background. The fit to salinity, on the other hand, shows very little improvement over the FR background. The error in salinity, especially during September, is large with J_{fit} values exceeding 6. A further check of these observations shows that a majority of them are located near the northern Gulf Coast, in the Mississippi River outflow region; these observations near the northern Gulf Coast are more numerous in the month of September. These specific salinity observations exhibit large innovations when compared to the free-run solution (some greater than 3.0 psu). This is likely due to poorly

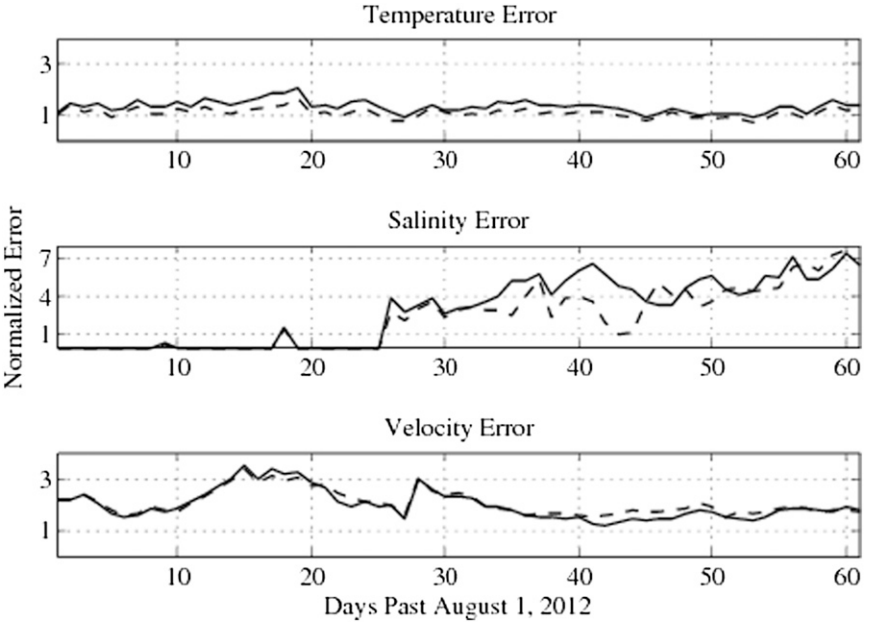

FIG. 4. As in Fig. 3, but for nonassimilated observations.

specified river inflow information in the model combined with incorrect near-surface ocean currents, as seen in the velocity J_{fit} values in Fig. 4. It is important to note that the J_{fit} values are normalized by the assumed observation error, which in this case is 0.1 psu for salinity. This factor, combined with the large innovations, results in a large J_{fit} value for salinity.

Examining the forecasts generated from the 4DVAR analysis in the TS experiment can be done by computing the skill score relative to the FR forecast. The skill score is a measure of the relative root-mean-square (RMS) error in one forecast solution to another. Here, the RMS error for the TS and FR forecasts are computed by using all of the available temperature, salinity, and velocity observations valid during the forecast period:

$$\text{RMS} = \sqrt{\frac{1}{M}\sum_{m=1}^{M}(\mathbf{y}_m - H_m\mathbf{x}^f)^2} \qquad (6)$$

where M is the total number of observations, $\mathbf{y}_m$ is the mth observation, and $\mathbf{x}^f$ is the model forecast solution. It should be noted that the observations used to compute the RMS error have not yet been assimilated as they are compared here to the forecast, not the analysis; in this regard, the data used in this comparison are independent observations. The skill score is then computed by comparing the RMS error of the TS and FR forecasts as

$$\text{SS} = 1.0 - \frac{\text{RMS}_{\text{TS}}}{\text{RMS}_{\text{FR}}}. \qquad (7)$$

Equation (7) shows that if the RMS error of the TS forecast is lower (higher) than the FR forecast, the skill score metric will be positive (negative). If there is no change, the skill score value should be nearly zero. Figure 5 shows the computed skill score from the TS experiment, relative to the FR solution, for each of the 96-h forecasts generated from the 4DVAR analyses every 4 days for temperature (top panel), salinity (middle panel), and velocity (bottom panel) from 1 August to 30 September 2012 (solid line shows the skill score value, dashed line indicates zero skill score value). Figure 5 shows that the TS solution produces an improved forecast in temperature and salinity during most of the experiment time frame over that of the FR solution. For salinity, the TS experiment generally outperforms FR in September, with a few exceptions. There is almost no improvement whatsoever in the velocity forecast. This is not surprising given the analysis results shown in Figs. 3 and 4. Figure 5 suggests that the assimilation of temperature and salinity alone does not constrain the model solution enough in terms of the surface velocities.

Adding the GLAD-derived drifter velocity observations to the assimilation is done in the ALL experiment. One concern that exists when combining multiple observation types in the same 4DVAR minimization is that one or more data types will be fit by the analysis at the expense of another data type. There are many reasons why this could occur, but is usually due to the relative errors of each data type, the size of the innovations and their contribution to the cost function, and the criteria

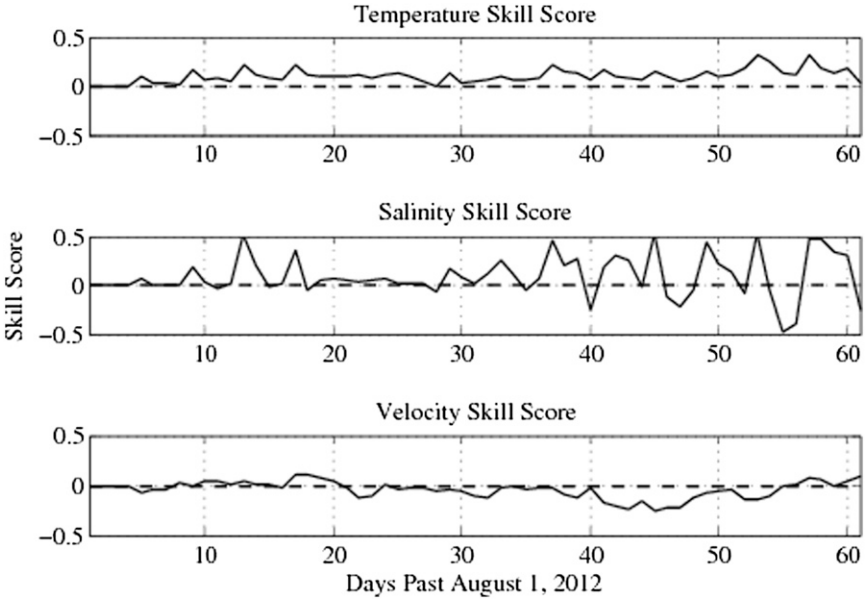

FIG. 5. TS forecast skill score values, measured against NCOM free-run solution for (top) temperature, (middle) salinity, and (bottom) velocity. Valid from 1 Aug to 30 Sep 2012. Skill score indicated by the solid line and zero skill score value indicated by the dashed line.

for the convergence of the conjugate gradient algorithm. Temperature observations, in particular, can be numerous (especially at the surface) in comparison to other data types and can often have larger innovations than salinity or ocean velocities. Therefore, if the convergence criterion is less strict, the algorithm may converge having only fitted temperature observations properly. For this reason, the analysis fit to temperature, salinity, and velocity is compared to the TS analysis in Fig. 6. This figure shows the J_{fit} value to determine the impact of the

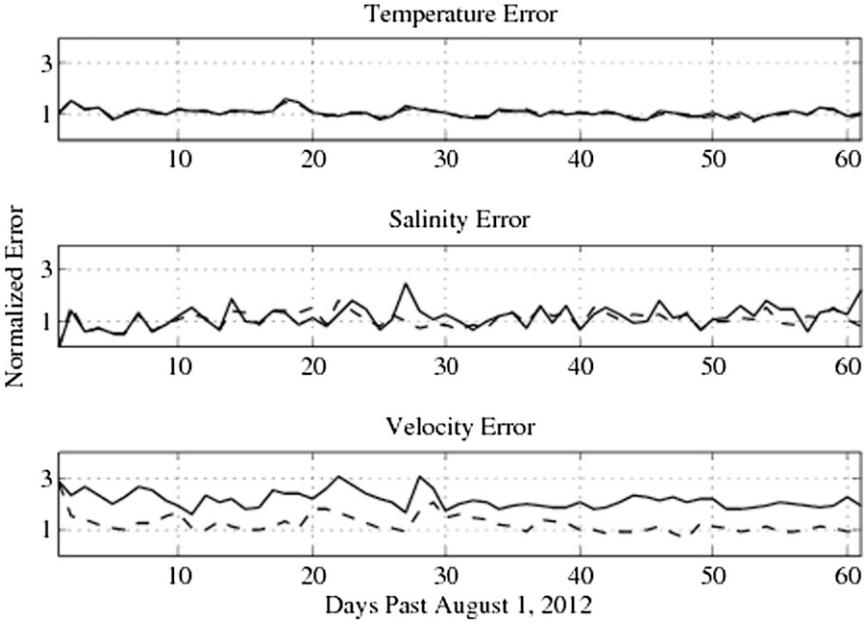

FIG. 6. The J_{fit} metric values for the TS analysis solution (solid line) and ALL analysis solution (dashed line) measured against (top) assimilated temperature observations, (middle) salinity observations, and (bottom) GLAD velocity observations. Valid from 1 Aug to 30 Sep 2012.

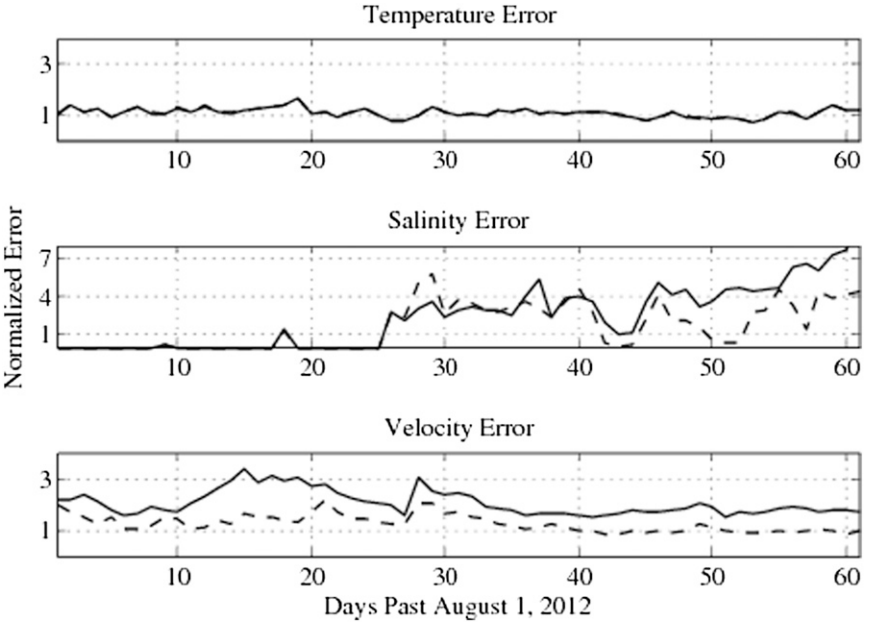

FIG. 7. As in Fig. 6, but for nonassimilated observations.

observations on this analysis and compares the analysis error in temperature (top panel), salinity (middle panel), and velocity (bottom panel) from the TS experiment (solid) and the ALL experiment (dashed). Here, it is seen that the ALL experiment continues to fit the temperature and salinity observations well, nearly matching the results from the TS experiment (doing marginally better, in fact, than the TS analysis in terms of salinity). This indicates that the inclusion of the surface velocity data type in the analysis has not degraded the analysis fit to the other assimilated data types.

Figure 6 also shows that the assimilation of surface velocity from the GLAD drifter data has greatly improved the analysis fit to these observations over the TS analysis. It can be seen that the ALL experiment fits the velocity observations to within the prescribed error through the last month of the experiment, although it does have some trouble with the fit earlier through the month of August. This is likely due to the model analysis and forecast adjusting to the surface currents during the earlier portion of the experiment.

As with the comparison of the TS analysis and FR background, the J_{fit} values for the TS and ALL analyses using the withheld observations are computed; Fig. 7 shows this comparison. The J_{fit} value for temperature indicates that the ALL analysis (dashed) fits the withheld temperature observations just as well as the TS analysis (solid). In addition to this, the ALL analysis shows an improved fit to the withheld salinity observations when compared to the TS analysis. This suggests that the assimilation of GLAD velocity observations near the northern Gulf Coast is helping to constrain the salinity gradients near the Mississippi River outflow region, which results in a better fit to these independent observations. The ALL analysis fit to withheld GLAD velocity observations also shows improvement over the TS analysis, even fitting the withheld observations to within the prescribed data error during the latter half of the experiment run.

Figure 8 examines the observation minus analysis misfit, spatially, and by velocity component from 1 August to 30 September for the u component (left panels) and v component (right panels) from the TS analysis (top panels) and ALL analysis (bottom panels); observation minus analysis misfits are plotted daily for ease of viewing. Clearly, the ALL analysis fits the GLAD velocity data better than the TS experiment, with most of the misfit values near zero. The TS analysis appears to have higher error in the central Gulf of Mexico in the vicinity of the loop current eddy. The ALL analysis appears to have reduced this error significantly and has a better representation of the velocity field in the central Gulf of Mexico than the TS analysis.

It has now been shown that the inclusion of velocity observations leads to an improved surface velocity representation (according to available observations) than without velocity assimilation. To see the impact of these observations on the subsequent forecast, Fig. 9 displays the forecast skill score of the ALL 96-h forecasts, relative to the TS forecasts using (7) for temperature (top panel),

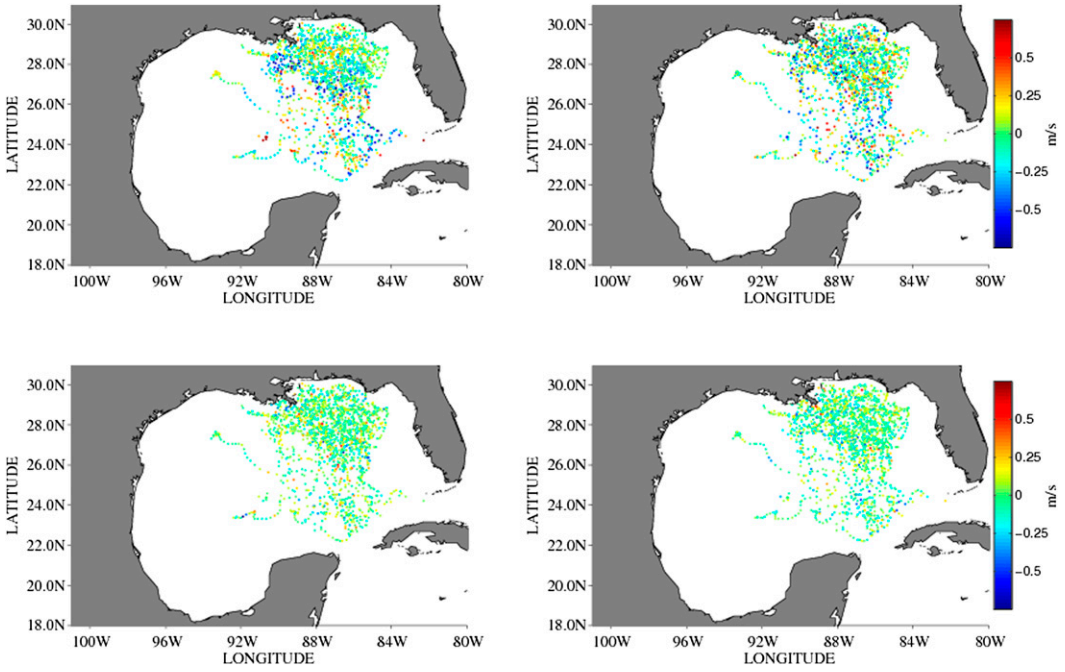

FIG. 8. GLAD velocity observation (top) minus TS analysis solution and (bottom) minus ALL analysis solution for the (left) u component and (right) v component of velocity. Difference values plotted daily from 1 Aug to 30 Sep 2012. Difference values in m s^{-1} (magnitude indicated by the color bar).

salinity (middle panel), and velocity (bottom panel). The ALL forecast of temperature is just as good as the TS solution, indicating that the ALL forecast is also producing an improved temperature field over the FR solution (as in the TS experiment). Interestingly, the ALL forecast of salinity shows a significant improvement over the TS forecast, especially through the month of September. This is consistent with the results in Fig. 7

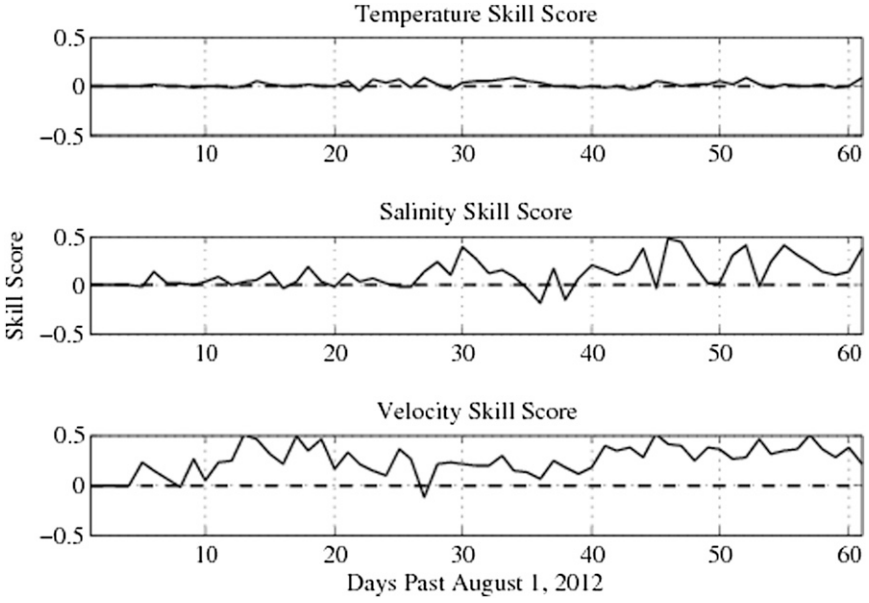

FIG. 9. ALL forecast skill score values, measured against TS forecast solution for (top) temperature, (middle) salinity, and (bottom) velocity. Valid from 1 Aug to 30 Sep 2012. Skill score indicated by the solid line and zero skill score value indicated by the dashed line.

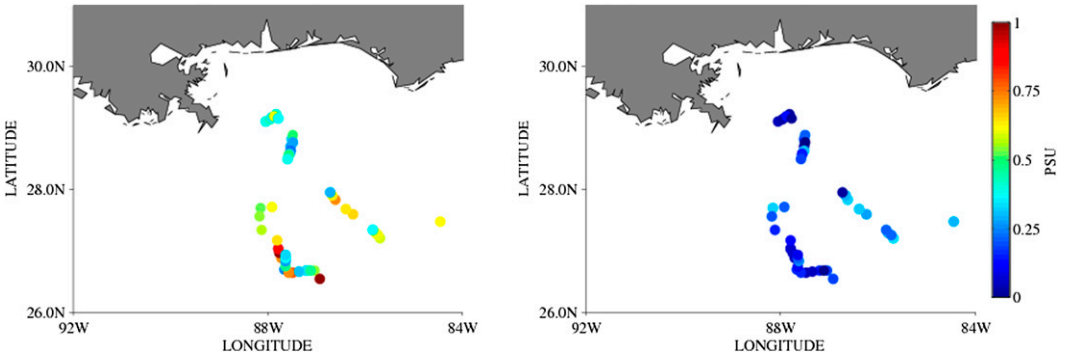

FIG. 10. Observed salinity values minus (right) TS forecast solution and (left) ALL forecast solution, valid between 10 and 30 Sep 2012 (values in psu, indicated by color bar). NCOM model forecast fields are mapped to the observed location at the appropriate time.

that showed the ALL analysis fit the withheld salinity observations better than the TS analysis. This result suggests that the better fit to withheld salinity observations, along with the improved surface current representation, in the ALL analysis has helped to improve the prediction of salinity in the ALL forecast relative to the TS experiment. The bottom panel in Fig. 9 displays the forecast skill score for the velocity field from the ALL experiment relative to the TS experiment. The skill score is well above zero for the majority of the experiment time frame, indicating that the improved velocity analysis in the ALL experiment does indeed translate to an improved forecast when compared to the TS experiment. The improvement gained by the assimilation of the GLAD velocity observations generally lasts the entirety of each 96-h forecast, indicating that the improvement is not short lived and the memory of the information gained from the assimilation in the forecast is significant.

Examining the salinity forecast in TS and ALL more closely, the majority of the improvement in the skill score in Fig. 9 is from near-surface salinity observations near the northern Gulf Coast. Figure 10 shows the absolute difference between a set of near-surface salinity observations and the TS salinity forecast (left panel) and ALL salinity forecast (right panel) for the period of 10–30 September 2012 in a subset region from the NCOM domain near the northern Gulf Coast (absolute difference value indicated by the color bar). It is clear from Fig. 10 that the ALL salinity forecast is matching the observations much more closely than the TS forecast. Further examining the forecast salinity within the same region as Fig. 10 (with surface velocities overlaid) from 25 September 2012 from TS (Fig. 11, left panel) and ALL (Fig. 11, right panel) shows significant differences in the two forecast salinity fields. The salinity forecast from TS shows higher salinity values south of 28°N with the freshest water associated with the Mississippi River outflow confined nearest the coast. This differs from the ALL salinity forecast, which shows generally lower salinity values south of 28°N, with an offshore eddy (centered at 26.5°N, 91°W) driving a current that is pulling freshwater from the Mississippi River outflow farther away from the coast into the central Gulf. It was shown in Fig. 10 that the ALL surface currents are more accurate

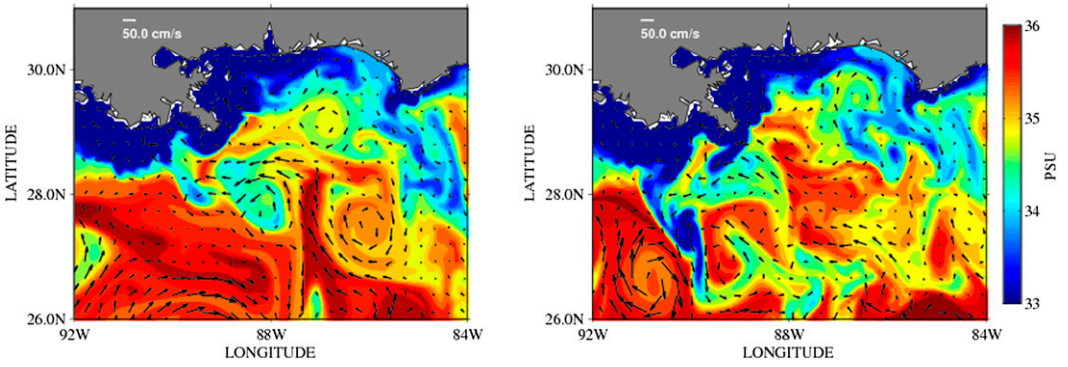

FIG. 11. (left) TS forecast salinity field and (right) ALL forecast salinity field, with surface velocity field overlaid (vector plots), valid 25 Sep 2012.

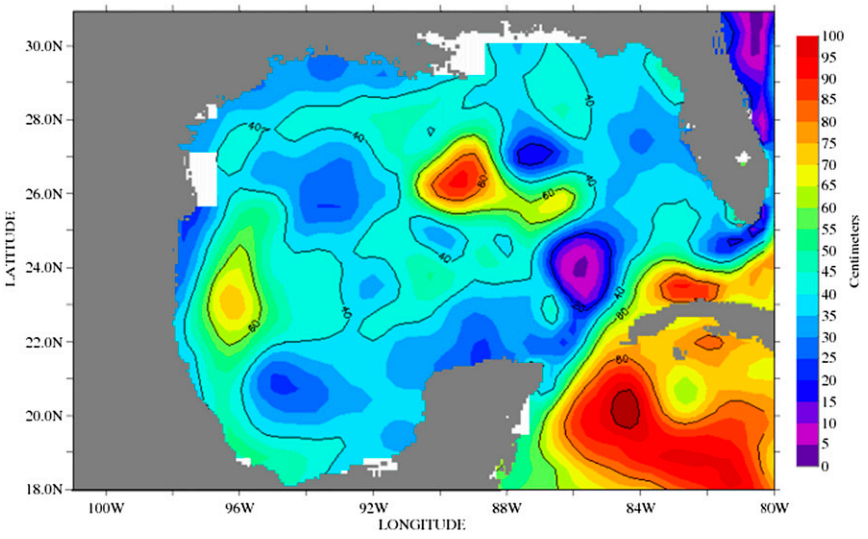

FIG. 12. Absolute dynamic height (ADH) from the AVISO product (this altimeter product was produced by Ssalto/*Duacs* and distributed by AVISO, with support from CNES at http://www.aviso.oceanobs.com/duacs/), valid 22 Aug 2012.

than TS (when compared to the GLAD velocity observations), and this region is covered quite well by the GLAD drifters during this time frame, suggesting that the surface currents seen in the ALL forecast in Fig. 11 are likely more accurate than those of the TS forecast. Therefore, it is likely that the improved near-surface velocity forecast in ALL is driving the improved salinity forecast when compared to the TS solution.

The assimilation of velocity observations can also help improve the mesoscale eddy representation in the model. This is due to the dynamical balance relationship provided by the tangent linear and adjoint of the ocean model; corrections to the surface velocity field can lead to an improvement in the model surface elevation field. Figures 12, 13, and 14 show the comparison of absolute dynamic height (ADH; in meters) from the Archiving, Validation, and Interpretation of Satellite Oceanographic data (AVISO) product [this altimeter product was produced by the Segment Sol multimissions d'Altimétrie, d'Orbitographie et de localisation precise (Ssalto)/*Data Unification and Altimeter Combination System* (*Duacs*) and distributed by AVISO, with support from the Centre National d'Études Spatiales (CNES) at http://www.aviso.oceanobs.com/duacs/; Fig. 12], the TS

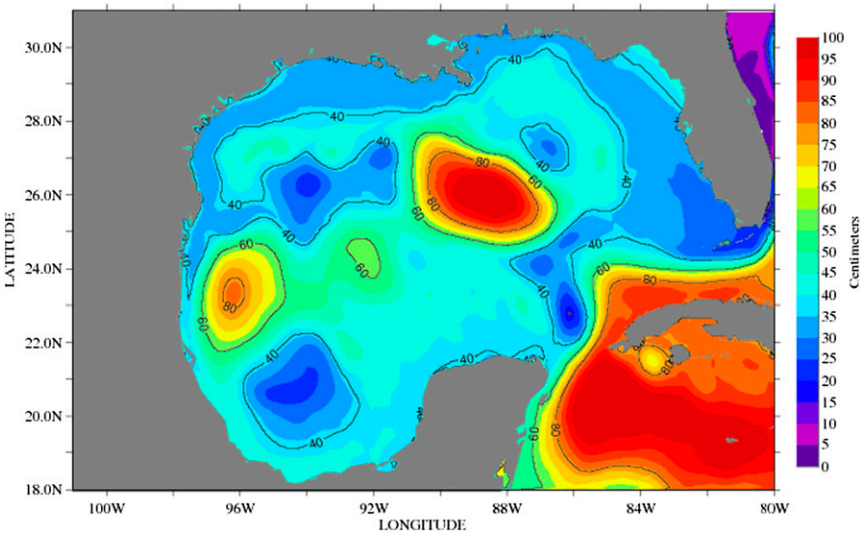

FIG. 13. As in Fig. 12, but for absolute dynamic height from the TS forecast solution.

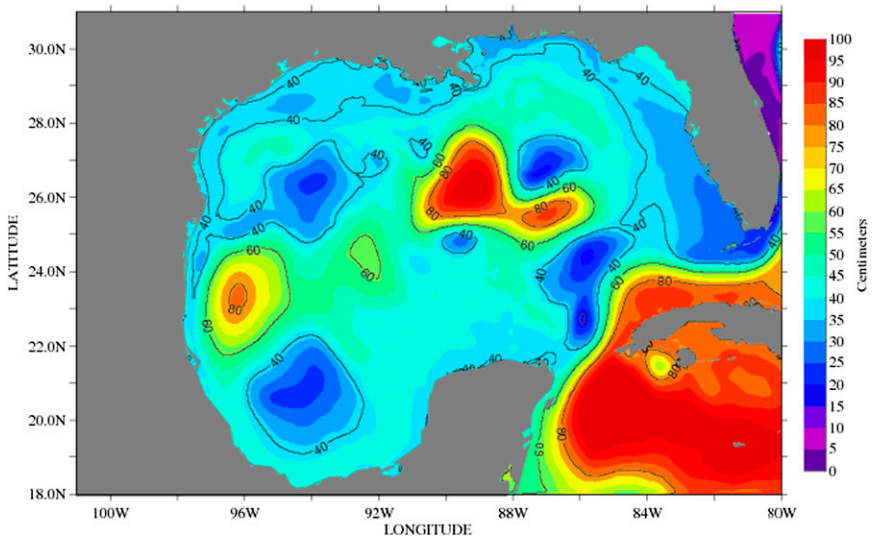

FIG. 14. As in Fig. 12, but for absolute dynamic height from the ALL forecast solution.

experiment (Fig. 13), and the ALL experiment (Fig. 14), valid on 22 August 2012. When comparing TS and ALL to the AVISO product in the region bounded by 22°–30°N, 84°–92°W (i.e., the region covered by dense GLAD velocity observations), there is a stark contrast between the two model solutions. The TS ADH field exhibits one large, elliptic eddy feature south of the Mississippi River delta. This differs from the AVISO product that indicates the eddy structure is smaller with an elongated ''tongue'' of high ADH extending to the south and east of the primary eddy (with regions of lower ADH to the north and south of this tongue). The ADH field from the ALL forecast exhibits an eddy structure much closer to the AVISO product than does the TS forecast. The ALL ADH field shows the same tongue structure with the lower ADH regions north and south as in the AVISO product, albeit with higher overall height values. This indicates that the assimilation of surface velocity measurements from GLAD has helped to constrain the surface eddy field in the vicinity of the drifter observations. An examination of other time periods throughout the ALL experiment show similar agreement with the AVISO product (figures not shown).

6. Summary

The assimilation of surface velocity observations, derived from GLAD drifter positions, within the weak-constraint NCOM-4DVAR has been shown. By comparing the assimilation results in terms of the analysis fit to the observations, as well as the subsequent forecast fit to future observations between an experiment with no velocity assimilation (TS) and an experiment with velocity assimilation (ALL), we have been able to conclude that assimilating the surface velocity observations leads to a substantial improvement in not only the analysis fit, but also in the forecast as well. The assimilation of velocity observations also led to an improved salinity forecast, as shown in the comparison of the results from the ALL and TS experiments. This is likely due to the fact that the assimilation of GLAD velocity observations near the northern Gulf Coast is helping to constrain the salinity gradients near the Mississippi River outflow region, resulting in a better fit to these salinity observations in that region. The forecast skill score of the ALL forecast relative to the TS forecast shows that the information gained in the assimilation of velocity observations is not short lived, with improvement in the velocity forecast in ALL over the TS experiment shown to remain out to 96 h. It was also shown that the assimilation of surface velocity measurements can improve the model representation of the surface elevation field. A comparison to the AVISO absolute dynamic height product shows that the ALL experiment captures the mesoscale eddy structure more accurately than the TS experiment in the vicinity of the velocity measurements. In short, it was shown that the assimilation of temperature and salinity observations alone in the 4DVAR does not properly constrain the model representation of the surface flow field in the Gulf of Mexico. The results of this study suggest that surface velocity measurements can be used to help constrain the model flow field and, therefore, the mesoscale eddy structures. Assimilating surface velocity information can help to correct the model representation of the surface elevation field as well as help to constrain the

tracer fields, specifically the surface salinity. The results shown in this study suggest that surface velocity observations can have a profound impact on the model solution, not only on the representation of the flow field, but across other ocean variables as well.

Now that the assimilation of surface velocity observations has been shown to work well when the velocity observations take the Eulerian form, attention can be given to the Lagrangian assimilation of the GLAD drifter observations in their native Lagrangian form. To do this, the capability to evolve model drifters within the NCOM solution will be added in the near future. Once this is done, the NCOM-4DVAR can be used to minimize the distance between the model and observed drifter positions (using a suitable measurement functional), thereby propagating this information to the model Eulerian velocity fields in the analysis step. The results of a future Lagrangian data assimilation effort with GLAD data will be compared to this work to determine if there is any improvement in the accuracy of the velocity analysis and/or forecast over the pseudo-Lagrangian DA method, and if so, it will determine if the gain is substantial. This question will be investigated in a future experiment and subsequent paper.

Acknowledgments. The authors would like to acknowledge Emanuel Coelho for his work in processing the GLAD drifter observations into Eulerian velocity measurements used in this assimilation study. The authors would like to thank the anonymous reviewers for their helpful comments during the revision process. The authors would also like to state that this research was made possible in part by a grant from BP/The Gulf of Mexico Research Initiative (GoMRI) through the Consortium for Advanced Research on Transport of Hydrocarbon in the Environment (CARTHE). This work was also sponsored by the Office of Naval Research Program Element 0601153N as part of the projects ''A Multiscale Approach to Assessing Predictability of ASW Environment'' and ''The Rapid Transition Project (RTP) for 4Dvar NCOM in RELO and COAMPS5 with merged NCODA/NAVDAS-AR.''

REFERENCES

Barron, C. N., A. Birol Kara, P. J. Martin, R. C. Rhodes, and L. Smedstad, 2006: Formulation, implementation and examination of vertical coordinate choices in the Global Navy Coastal Ocean Model (NCOM). *Ocean Modell.,* **11,** 347–375, doi:10.1016/j.ocemod.2005.01.004.

Bennett, A. F., 1992: *Inverse Methods in Physical Oceanography.* Cambridge University Press, 347 pp.

——, 2002: *Inverse Modeling of the Ocean and Atmosphere.* Cambridge University Press, 234 pp.

Bleck, R., 2002: An oceanic general circulation model framed in hybrid isopycnic-Cartesian coordinates. *Ocean Modell.,* **4,** 55–88, doi:10.1016/S1463-5003(01)00012-9.

Blumberg, A. F., and G. L. Mellor, 1987: A description of a three-dimensional coastal ocean circulation model. *Three-Dimensional Coastal Ocean Models,* N. Heaps, Ed., Amer. Geophys. Union, 1–16.

Carrier, M. J., and H. Ngodock, 2010: Background-error correlation model based on the implicit solution of a diffusion equation. *Ocean Modell.,* **35,** 45–53, doi:10.1016/j.ocemod.2010.06.003.

Chua, B. S., and A. F. Bennett, 2001: An inverse ocean modeling system. *Ocean Modell.,* **3,** 137–165, doi:10.1016/S1463-5003(01)00006-3.

Courtier, P., 1997: Dual formulation of four-dimensional variational assimilation. *Quart. J. Roy. Meteor. Soc.,* **123,** 2449–2461, doi:10.1002/qj.49712354414.

Cummings, J. A., 2005: Operational multivariate ocean data assimilation. *Quart. J. Roy. Meteor. Soc.,* **131,** 3583–3604, doi:10.1256/qj.05.105.

Fan, S., O. Lie-Yauw, and P. Hamilton, 2004: Assimilation of drifter and satellite data in a model of the northeastern Gulf of Mexico. *Cont. Shelf Res.,* **24,** 1001–1013, doi:10.1016/j.csr.2004.02.013.

Hernandez, F., P. Y. Le Traon, and N. H. Barth, 1995: Optimizing a drifter cast strategy with a genetic algorithm. *J. Atmos. Oceanic Technol.,* **12,** 330–345, doi:10.1175/1520-0426(1995)012<0330:OADCSW>2.0.CO;2.

Ide, K., L. Kuznetsov, and C. K. R. T. Jones, 2002: Lagrangian data assimilation for point vortex systems. *J. Turbul.*, **3**, 053, doi:10.1088/1468-5248/3/1/053.

Ishikawa, Y. I., T. Awaji, and K. Akimoto, 1996: Successive correction of the mean sea surface height by the simultaneous assimilation of drifting buoy and altimetric data. *J. Phys. Oceanogr.,* **26,** 2381–2397, doi:10.1175/1520-0485(1996)026<2381:SCOTMS>2.0.CO;2.

Kurapov, A. L., G. D. Egbert, J. S. Allen, and R. N. Miller, 2009: Representer-based analyses in the coastal upwelling system. *Dyn. Atmos. Oceans,* **48** (1–3), 198–218, doi:10.1016/j.dynatmoce.2008.09.002.

——, D. Foley, P. T. Strub, G. D. Egbert, and T. S. Allen, 2011: Variational assimilation of satellite observations in a coastal ocean model off Oregon. *J. Geophys. Res.,* **116,** C05006, doi:10.1029/2010JC006909.

Kuznetsov, L., K. Ide, and C. K. R. T. Jones, 2003: A method for assimilation of Lagrangian data. *Mon. Wea. Rev.,* **131,** 2247–2260, doi:10.1175/1520-0493(2003)131<2247:AMFAOL>2.0.CO;2.

Marchesiello, P., J. C. McWilliams, and A. F. Shchepetkin, 2001: Open boundary conditions for long-term integration of regional oceanic models. *Ocean Modell.,* **3,** 1–20, doi:10.1016/S1463-5003(00)00013-5.

Martin, P. J., 2000: Description of the Navy Coastal Ocean Model version 1.0. NRL Rep. NRL/FR/7322/00/9962, 45 pp. [Available from NRL, Code 7322, Bldg. 1009, Stennis Space Center, MS 39529-5004.]

Mellor, G. L., and T. Yamada, 1982: Development of a turbulence closure model for geophysical fluid problems. *Rev. Geophys. Space Phys.,* **20,** 851–875, doi:10.1029/RG020i004p00851.

Molcard, A., L. I. Piterbarg, A. Griffa, T. M. Ozgokmen, and A. J. Mariano, 2003: Assimilation of drifter positions for the reconstruction of the Eulerian circulation field. *J. Geophys. Res.,* **108,** 3056, doi:10.1029/2001JC001240.

——, A. Griffa, and T. M. Ozgokmen, 2005: Lagrangian data assimilation in multilayer primitive equation ocean models. *J. Atmos. Oceanic Technol.,* **22,** 70–83, doi:10.1175/JTECH-1686.1.

Ngodock, H. E., 2005: Efficient implementation of covariance multiplication for data assimilation with the representer method. *Ocean Modell.,* **8,** 237–251, doi:10.1016/j.ocemod.2003.12.005.

——, and M. J. Carrier, 2013: A weak constraint 4D-Var Assimilation system for the Navy coastal ocean model using the representer method. *Data Assimilation for Atmospheric, Oceanic and Hydrologic Applications, Vol. II,* S. K. Park and L. Xu, Eds., Springer-Verlag, 367–390, doi:10.1007/978-3-642-35088-7_15.

Nilsson, J. A. U., S. Dobricic, N. Pinardi, P. M. Poulain, and D. Pettenuzzo, 2012: Variational assimilation of Lagrangian trajectories in the Mediterranean Ocean forecasting system. *Ocean Sci.,* **8** (2), 249–259, doi:10.5194/os-8-249-2012.

Ozgokmen, T. M., A. Molcard, T. M. Chin, L. I. Piterbarg, and A. Griffa, 2003: Assimilation of drifter positions in primitive equation models of midlatitude ocean circulation. *J. Geophys. Res.,* **108,** 3238, doi:10.1029/2002JC001719.

Roemmich, D., and Coauthors, 2001: Argo: The global array of profiling floats. *Observing the Oceans in the 21st Century,* C. J. Koblinsky and N. R. Smith, Eds., Melbourne Bureau of Meteorology, 248–257.

Rosmond, T. E., J. Teixeria, M. Peng, T. F. Hogan, and R. Pauley, 2002: Navy operational global prediction system (NOGAPS): Forcing for ocean models. *Oceanography,* **15,** 99–106, doi:10.5670/oceanog.2002.40.

Salman, H., L. Kuznetsov, and C. K. R. T. Jones, 2006: A method for assimilating Lagrangian data into a shallow-water-equation ocean model. *Mon. Wea. Rev.,* **134,** 1081–1101, doi:10.1175/MWR3104.1.

Shchepetkin, A. F., and J. C. McWilliams, 2003: A method for computing horizontal pressure-gradient force in an oceanic model with nonaligned vertical coordinate. *J. Geophys. Res.,* **108,** 3090, doi:10.1029/2001JC001047.

——, and ——, 2005: The regional oceanic modeling system (ROMS): A split-explicit, free-surface, topography-following-coordinate oceanic model. *Ocean Modell.,* **9,** 347–404, doi:10.1016/j.ocemod.2004.08.002.

Smagorinsky, J., 1963: General circulation experiments with the primitive equations. I: The basic experiment. *Mon. Wea. Rev.,* **91,** 99–164, doi:10.1175/1520-0493(1963)091<0099:GCEWTP>2.3.CO;2.

Taillandier, V., A. Griffa, and A. Molcard, 2006: A variational approach for the reconstruction of regional scale Eulerian velocity fields from Lagrangian data. *Ocean Modell.,* **13,** 1–24, doi:10.1016/j.ocemod.2005.09.002.

Weaver, A. T., and P. Courtier, 2001: Correlation modeling on the sphere using a generalized diffusion equation. *Quart. J. Roy. Meteor. Soc.,* **127,** 1815–1846, doi:10.1002/qj.49712757518.

Yaremchuk, M., M. Carrier, S. Smith, and G. Jacobs, 2013: Background error correlation modeling with diffusion operators. *Data Assimilation for Atmospheric, Oceanic and Hydrologic Applications, Vol II,* S. K. Park and L. Xu, Eds., Springer-Verlag, 177–203, doi:10.1007/978-3-642-35088-7_8.

Yu, P., A. L. Kurapov, G. D. Egbert, J. S. Allen, and A. P. Kosro, 2012: Variational assimilation of HF radar surface currents in a coastal ocean model off Oregon. *Ocean Modell.,* **49–50,** 86–104, doi:10.1016/j.ocemod.2012.03.001.